

Manuscript Number: SMM-17-2109

Title: Thermoelectric properties and cost optimization of spark plasma sintered n-type Si_{0.9}Ge_{0.1} - Mg₂Si nanocomposites

Article Type: Regular article

Keywords: Thermoelectric materials; spark plasma sintering; mechanical alloying; silicon germanium; nanocomposite.

Corresponding Author: Mr. Andrey Usenko, Ph.D

Corresponding Author's Institution:

First Author: Andrey Usenko, Ph.D

Order of Authors: Andrey Usenko, Ph.D; Dmitry Moskovskikh, Ph.D; Andrey Korotitskiy, Ph.D; Mikhail Gorshenkov, Ph.D; Elena Zakharova; Aleksandr Fedorov, Ph.D; Yury Parkhomenko, Ph.D; Vladimir Khovaylo, Ph.D

Abstract: We report on thermoelectric properties of low Ge content n-type Si_{0.9}Ge_{0.1}-Mg₂Si nanocomposite. Introduction of the Mg₂Si phase into a SiGe matrix resulted in a dramatic drop of the lattice thermal conductivity beyond the previously reported lowest limit for SiGe alloys due to intensification of phonon scattering on SiGe-Mg₂Si grain boundaries. For a sample doped with 1 at.% of Mg₂Si, the peak value of thermoelectric figure of merit ZT reached ~ 0.8 at 800°C. Sintered nanocomposites still exhibit high thermoelectric performance while being almost two times cheaper than Si_{0.8}Ge_{0.2}.

Suggested Reviewers: Takao Mori PhD
National Institute for Materials Science
MORI.Takao@nims.go.jp

One of the most experienced scientists in the field of high temperature thermoelectrics

Anatolie Casian PhD
Technical University of Moldova
acasian@mail.utm.md

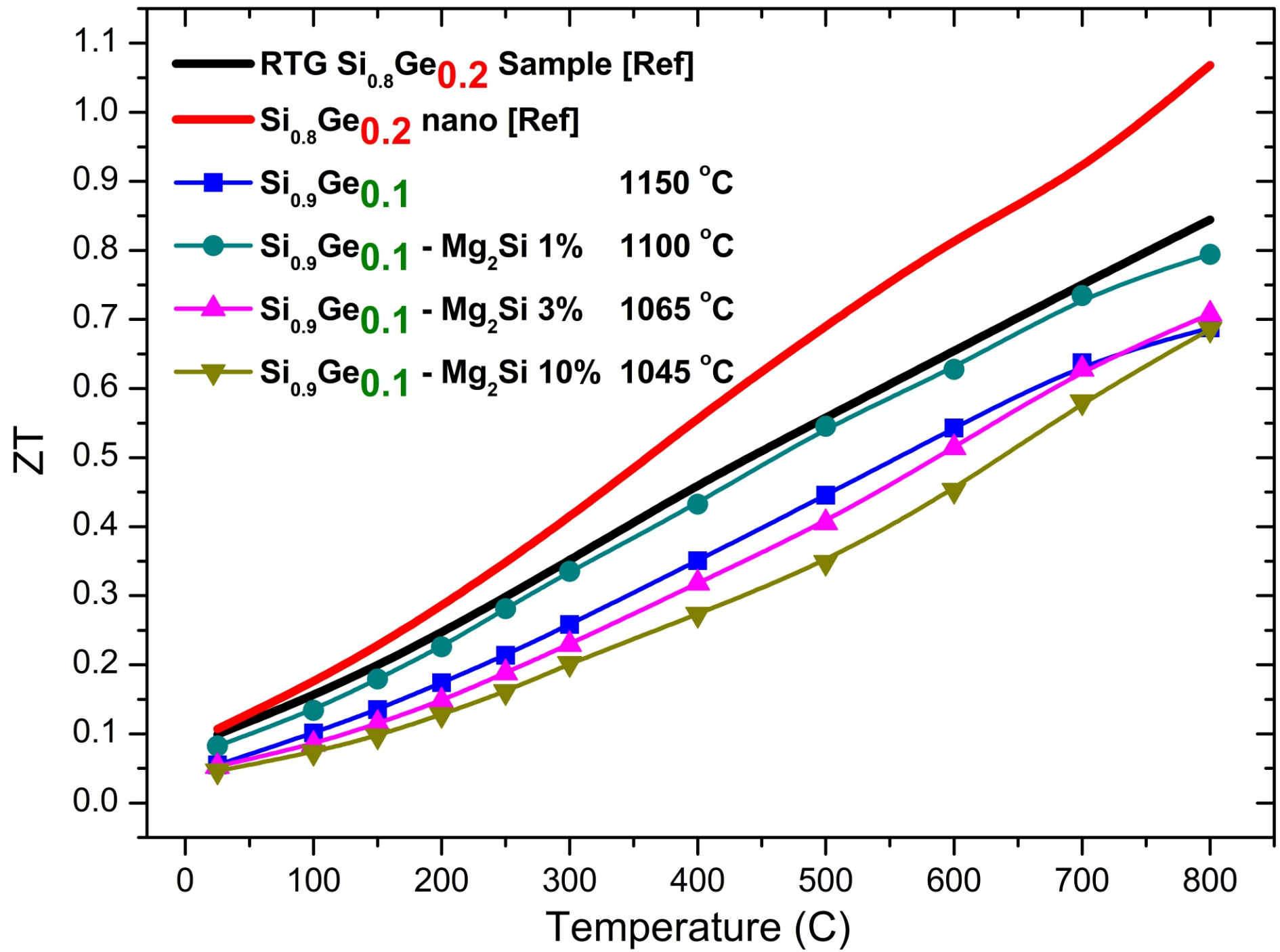
Aleksandr Trofimovich Burkov PhD
Professor, Ioffe Physical Technical Institute, Russian Academy of Science
a.burkov@mail.ioffe.ru
Board of European thermoelectric society

Andriy Grytsiv PhD
University of Vienna
andriy.grytsiv@univie.ac.at

Yuri Gurevich PhD
National Polytechnic Institute
gurevich@fis.cinvestav.mx

Cover letter

The aim of our work was to investigate thermoelectric figure of merit of *n*-type $\text{Si}_{0.9}\text{Ge}_{0.1}\text{-Mg}_2\text{Si}$ nanocomposites with a respect of Mg_2Si content. It was demonstrated that high ZT values can be achieved in high dense composite structures which is maintain high values of the electrical conductivity. This study highlights that the nanocomposites with low Ge content could have competitive ZT values as well as being cost effective.



Material cost optimization

Ge content decreased by 100 %
compare to conventional
SiGe thermoelectric materials

Material cost  ~ 90%

ZT Value  ~ 5 - 10%

Thermoelectric properties and cost optimization of spark plasma sintered *n*-type Si_{0.9}Ge_{0.1} - Mg₂Si nanocomposites

Andrey Usenko¹, Dmitry Moskovskikh¹, Andrey Korotitskiy¹, Mikhail Gorshenkov¹, Elena Zakharova¹, Aleksandr Fedorov^{2,3}, Yury Parkhomenko¹, and Vladimir Khovaylo^{1,4}

¹National University of Science and Technology "MISIS", Moscow 119049, Russia

²Siberian Federal University, Krasnoyarsk 660041, Russia

³Kirensky Institute of Physics, Krasnoyarsk 660036, Russia

⁴National Research South Ural State University, Chelyabinsk 454080, Russia

Keywords:

Thermoelectric materials; spark plasma sintering; mechanical alloying; silicon; germanium; magnesium silicide; nanocomposite.

Abstract

We report on thermoelectric properties of low Ge content *n*-type Si_{0.9}Ge_{0.1}-Mg₂Si nanocomposite. Introduction of the Mg₂Si phase into a SiGe matrix resulted in a dramatic drop of the lattice thermal conductivity beyond the previously reported lowest limit for SiGe alloys due to intensification of phonon scattering on SiGe-Mg₂Si grain boundaries. For a sample doped with 1 at.% of Mg₂Si, the peak value of thermoelectric figure of merit *ZT* reached ~ 0.8 at 800°C. Sintered nanocomposites still exhibit high thermoelectric performance while being almost two times cheaper than Si_{0.8}Ge_{0.2}.

It is well known that thermoelectric (TE) materials such as silicon germanium alloys have been used in radioisotope thermoelectric generators (RTG) for NASA space missions [1]. High mechanical strength and resistance to atmospheric oxidation make this material suitable for a number of practical applications [1,2]. It has been demonstrated that SiGe alloys can be effectively used as a high temperature stage for cascade thermoelectric generators and less effectively in segmented generators due to their low compatibility factor [3–5]. Thermoelectric efficiency of any material is determined by dimensionless figure of merit, $ZT = \frac{S^2\sigma T}{k}$, where *S* is Seebeck coefficient, σ is electrical conductivity and *k* is thermal conductivity [1]. Recent progress in increasing *ZT* has been mainly driven by a reduction of thermal conductivity via nanostructuring approach [6–14]. It has been demonstrated that thermal and electrical transport is influenced by crystallite boundary scattering. If the crystallite sizes in a nanostructured material are comparable with the phonon mean free path but are larger than the charge carrier mean free path, thermal conductivity is reduced more

1 significantly than the electrical conductivity and this finally results in enhancement of ZT value. By
2 employing a similar approach, the authors have earlier reported a high value of $ZT = 1.05$ for n -type
3 nanostructured SiGe alloys by using spark plasma sintering of mechanically alloyed fine powders
4 [15].
5
6

7 Multiphase composite materials have been also considered for thermoelectric applications.
8 In 1999 Bergman and Fel have showed that composite material structures can improve the power
9 factor over the constituent components [16]. Later Mingo *et al.* [17] have performed electron and
10 phonon transport calculations for nanocomposites consisting of silicide nanoparticles embedded in a
11 SiGe matrix. They confirmed the previous studies that the thermal conductivity can be decreased
12 beyond the solid solution limit [18] via nanostructuring of the SiGe alloys to enhance ZT .
13 Furthermore, they discussed that silicide nanoinclusions can improve TE power factor of
14 nanocomposites through preferential scattering of the low energy charge carriers. Experimental
15 investigations have been performed for SiGe-based nanocomposites with the addition of FeSi₂,
16 CrSi₂, MoSi₂, and WSi₂ [19–23]. Previous results have showed that a significant reduction of
17 thermal conductivity is possible in silicide–SiGe nanocomposites as compared to polycrystalline or
18 nanostructured SiGe. The most significant boost of thermoelectric performance has been reported
19 by Ahmad *et al.* [24] for p -type SiGe–YSi₂ with $ZT \sim 1.81$ at 827 °C, which is ~34% higher as
20 compared to reported earlier the best values for p -type nanostructured SiGe. The authors have
21 explained such dramatic growth of ZT as due to the formation of a network of the coherent grain
22 boundaries at nanoscale in SiGe–YSi₂ by engineering at atomic scale. The coherent boundaries
23 effectively scatter phonons but allow charge carriers to pass through.
24
25
26
27
28
29
30
31
32
33
34
35
36
37

38 Recently, Nozariasbmarz *et al.* have reported on the very promising $ZT = 1.3$ at 900 °C for
39 n -type SiGe–Mg₂Si utilizing a smaller amount of germanium as compared to the RTG SiGe [25].
40 This would definitely be a significant achievement in the development of high temperature
41 thermoelectric converters with a lower cost and a higher efficiency. However, it must be noted that
42 dependence of ZT on sintering parameters as well as on the Mg₂Si content in SiGe–Mg₂Si
43 nanocomposites has not been studied in Ref. [25]. Moreover, reported by Nozariasbmarz *et al.*
44 sintering temperature $T = 1250$ °C of the studied SiGe–Mg₂Si nanocomposite is very peculiar in the
45 sense that it is almost 150 °C higher than the melting temperature of Mg₂Si. Generally, the liquid
46 phase sintering technique is very complicated, especially in the case of nanocomposites, because the
47 high internal stresses which can be generated by the melting of one of the nanocomposites'
48 component usually lead to the wrecking of the molding tools. The mentioned above concerns and a
49 high demand for the development of low cost – high efficiency thermoelectric materials motivated
50 us to an extended investigation of SiGe–Mg₂Si nanocomposites.
51
52
53
54
55
56
57
58
59
60
61
62
63
64
65

1 In this paper, *n*-type Si_{0.9}Ge_{0.1}–Mg₂Si nanocomposites were investigated with respect to the
2 Mg₂Si doping level and the results obtained were compared with the previously studied
3 nanostructured *n*-type Si_{0.8}Ge_{0.2} alloys [6]. The Ge content was decreased compared to conventional
4 Si_{0.8}Ge_{0.2} alloys in order to reduce the materials cost, since it was expected the lattice thermal
5 conductivity of nanocomposite k_L would be rather low despite the fact that k_L of crystalline
6 Si_{0.9}Ge_{0.1} is almost two times higher [18,26].
7
8
9

10 The raw chemical element Si, Ge, P of at least 99.99% purity and Mg₂Si powder (Alfa
11 Aesar) of 99.5% purity were used for preparation of the samples. First, Si, Ge and P were mixed in
12 desired proportions and ball milled in Fritsch 5 Pulverisette ball mill by using reference parameters
13 [7]. Then nanopowders of SiGe solid solution and Mg₂Si (~20 mesh) powder were mixed in desired
14 proportions and then ball milled in Frisch 7 Pulverisette ball mill. The vial of the ball mill and the
15 milling media were made of zirconium oxide. The ball-to-powder weight ratio was 20:1 and the
16 process was carried out in an argon atmosphere at a speed of 700 rpm. 1 wt. % of anti-friction and
17 re-welding control agent (alcohol) was added to the vials. The samples were sintered from the
18 powder using spark plasma sintering (SPS) technique (Labox 650, Sinter Land, Japan). The
19 powders were put into a cylindrical graphite die which was placed in a camera evacuated to a high
20 vacuum. Uniaxial pressure was then applied through top and bottom plungers. Each plunger has a
21 diameter of 12.7 mm and a length of 23 mm. The composite samples were prepared using the
22 following sintering conditions: the samples were compressed at room temperature for 1 minute,
23 then the pressure was risen up to 60 MPa; temperature of the samples was gradually raised to 1045
24 – 1100 °C depending on Mg₂Si content in the samples with a heating rate of 75°C/min; after the
25 soaking time of 5 minutes, the pressure was reduced to 10 MPa and the samples were cooled.
26 Experimental parameters of temperature, applied pressure, current, voltage, and sample
27 displacement were recorded simultaneously. Temperature was recorded by a thermocouple (Type
28 R) inserted in a hole drilled into the die surface to a depth of 3.5 mm. The compacted disc samples
29 have a dimension of 12.7 mm (diameter) × 2 mm (height). The samples were annealed at 900 °C
30 during one week. Microstructure of the samples was examined by scanning electron microscopy.
31 Elemental composition was analyzed by Energy Dispersive Spectroscopy (EDS). Studies of the
32 phase composition were carried out by Dron-2 X-ray diffractometer (Russia) at room temperature
33 using Co-K_α radiation ($\lambda = 1.79026 \text{ \AA}$). Density of the samples was determined by the Archimedes
34 technique. Thermal conductivity measurements were carried out using a laser flash analysis system
35 (Netzsch LFA 457) from room temperature up to 900 °C. Specific heat was measured by a
36 differential scanning calorimeter (DSC) Netzsch 204 F1. Electrical conductivity and Seebeck
37 coefficient were measured simultaneously on bars measuring 1×3×12 mm³ using a homemade
38
39
40
41
42
43
44
45
46
47
48
49
50
51
52
53
54
55
56
57
58
59
60
61
62
63
64
65

transport measuring system (Cryotel Ltd.) up to 800 °C. The accuracy of these measurements was checked against a silver sample of 99.99% purity.

Table 1 summarizes the sintering parameters and volume density of *n*-type Si_{0.9}Ge_{0.1} and Si_{0.9}Ge_{0.1}-Mg₂Si specimens. Sintering temperature of the nanocomposites was chosen with respect to Mg₂Si melting point –. Samples presented in this work were synthesized at temperatures below the melting temperature of Mg₂Si $T_m = 1102$ °C. However there were numerous attempts to synthesized nanocomposites by the so called liquid phase sintering technique (LPS) [27] to achieve higher values of volume density. These attempts were unsuccessful more likely due to poor wetting because of high values of contact angle between sintering components Even, below the melting temperature of Mg₂Si we faced with a local overheating due to SPS process that induced a local liquid phase formation and thereby led to high internal stresses that broke the samples. Thus the sintering temperature was decreased from 1100 °C to 1045 °C as the Mg₂Si content increased from 1% to 10% (Table 1). Figure 1 shows XRD patterns of *n*-type Si_{0.9}Ge_{0.1}-Mg₂Si 10% (at.) specimen: (a) mechanically alloyed SiGe nanopowder and Mg₂Si nanopowder mixture, (b) spark plasma sintered, (c) annealed at 900 °C. It is apparent from the figure that Ge completely dissolves in Si matrix after 2 hours of ball milling and Mg₂Si is maintained after the ball milling. The XRD peaks exhibit significant broadening because of the size effect and considerable amount of strains in nanopowder due to impact of shear forces of milling media during the high energy ball milling.

The possibility of retained nanograins for sintering temperature up to 1150 °C was previously demonstrated for bulk nanostructured Si_{0.8}Ge_{0.2} alloys [6,7,15]. Thus the growth of peak intensity is mainly attributed to the lattice strain sharp fall after SPS and subsequent annealing [28]. The elemental mapping of Si_{0.9}Ge_{0.1}-Mg₂Si 10% (at.) presented in Figure 2 confirms overall chemical homogeneity of the nanocomposite.

The main advantage of using SiGe nanostructuring approach for ZT enhancement is attributed to the fact that there is a large difference between mean free path of electrons and phonons: approximately 5 nm for electrons and 2 – 300 for phonons in highly doped samples at 25 °C [14]. Thus any nanostructure can reduce the phonon thermal conductivity without significant penalty for the electrical conductivity. Introducing Mg₂Si phase into SiGe matrix resulted in dramatic drop of lattice thermal conductivity that overcome the previous lowest limit for SiGe alloys due to intensification of phonon scattering on SiGe-Mg₂Si grain boundaries [19]. Figure 3a clearly shows that the prepared nanocomposites demonstrated a sharp drop of thermal conductivity as compared to the bulk RTG sample [1] and previously studied nanostructured *n*-type Si_{0.8}Ge_{0.2} alloy [6]. The achieved values of thermal conductivity 1.5 – 2.5 Wm⁻¹K⁻¹ are lower than those reported by Wang *et al.* [14], Bathula *et al.* [15] and Nozariasbmarz *et al.* [25]. The drop of thermal

1 conductivity was driven by: 1) intensification of phonon scattering on grain boundaries and 2) a
2 decrease of the volume density of the sintered samples with the increase of Mg₂Si content.

3
4 For further understanding of behavior of the thermal conductivity, the contributions from the
5 lattice thermal conductivity and from the electronic thermal conductivity were separated. The total
6 thermal conductivity is given by $k_{\text{total}} = k_e + k_L$ where k_e and k_L are the contributions to the thermal
7 conductivity from the carriers and the lattice, respectively. We calculate the electronic thermal
8 conductivity using the Wiedemann-Franz law $k_e/\sigma = LT$, where L – Lorenz number. The lattice
9 thermal conductivity was defined as the difference between total and electronic thermal
10 conductivity. Sintered nanocomposites demonstrated a linear behavior of the electronic thermal
11 conductivity (Figure 3b) which somewhat differs from that reported for the reference SiGe samples
12 [1,6]. As far as the reference samples are highly doped degenerate semiconductors the curve shape
13 demonstrated a non-monotonic behavior which is changed to linear at high temperatures due to an
14 increase of the intrinsic carrier concentration. The electronic contribution to the total thermal
15 conductivity correlated with the electrical conductivity and its influence on the total thermal
16 conductivity is rather weak. Figure 3c shows the significant drop of lattice thermal conductivity
17 down to $1.4 \text{ W m}^{-1} \text{ K}^{-1}$ for Si_{0.9}Ge_{0.1} - Mg₂Si 10% (at.) sample which indicates that the effect of grain
18 boundaries scattering in nanocomposite can compensate the lack of Ge in the SiGe matrix. The
19 lattice thermal conductivity reduced with the temperature due to enhancement of phonon-phonon
20 scattering.

21
22 Figure 4a shows temperature-dependent electrical conductivity. The electrical conductivity
23 values are strongly influenced by the chemical composition and the sintering temperature. The
24 behavior of the electrical conductivity is typical for highly doped semiconductors for Si_{0.9}Ge_{0.1} 1150
25 sample and Si_{0.9}Ge_{0.1}-Mg₂Si 1% (at.). In contrast, Si_{0.9}Ge_{0.1}-Mg₂Si 3% (at.) and Si_{0.9}Ge_{0.1}-Mg₂Si
26 10% (at.) specimens demonstrated nearly monotonic growth of the electrical conductivity that is
27 relevant for non-degenerate semiconductors. As it seen from figure 4a and figure 3a the electrical
28 conductivity is decreasing faster than the thermal conductivity with the decreasing sintering
29 temperature for the samples sintered at 1065 °C and 1045 °C. Thus the electrical conductivity of
30 Si_{0.9}Ge_{0.1}-Mg₂Si 10% (at.) dropped to $0.6 \cdot 10^4 \text{ Sm} \cdot \text{m}^{-1}$. The Seebeck coefficient absolute values
31 presented in Figure 4b demonstrated significant growth for all nanocomposite samples with the
32 increase of Mg₂Si content. This is more likely due to lower carrier concentration in nanocomposite
33 samples which also explains rather low values of the electrical conductivity. The ZT value of *n*-type
34 Si_{0.9}Ge_{0.1}-Mg₂Si nanocomposites follows the similar trend as that of RTG and previously studied
35 nanostructured sample (Figure 4c). Although the thermal conductivity of the studied
36
37
38
39
40
41
42
43
44
45
46
47
48
49
50
51
52
53
54
55
56
57
58
59
60
61
62
63
64
65

1 nanocomposites decreased dramatically, ZT remains almost equal to that of the RTG sample due to
2 simultaneous decrease of the power factor driven by fall of the electrical conductivity.

3 The thermoelectric properties of *n*-type Si_{0.9}Ge_{0.1}–Mg₂Si nanocomposites were studied in
4 the temperature range from 25 to 800 °C. Sintered nanocomposites demonstrated significant
5 decrease of the thermal conductivity down to 1.5 – 2.5 Wm⁻¹K⁻¹. The result can be explained by the
6 interface scattering mechanism for mid- to long- wavelength phonons, resulting in a further
7 reducing thermal conductivity that is lower than the alloy limit. The maximum ZT value reaches 0.8
8 at 800 °C for Si_{0.9}Ge_{0.1}–Mg₂Si 1% (at.), which is almost equal to RTG sample. This study highlights
9 that the nanocomposites with low Ge content could have competitive ZT values as well as being
10 cost effective. In order to enhance the ZT of current Si_{0.9}Ge_{0.1}–Mg₂Si nanocomposites new sintering
11 solution required to achieve higher dense structures to maintain high values of the power factor.
12
13
14
15
16
17
18
19
20

21 This work was supported by Russian Science Foundation (project No. 16-13-00060). Part of
22 the work (structural characterization of the samples) was carried out with financial support of the
23 Ministry of Education and Science of the Russian Federation in the framework of Increase
24 Competitiveness Program of NUST “MISiS”. Partial support by Act 211 Government of the
25 Russian Federation, contract # 02.A03.21.0011, is also acknowledged.
26
27
28
29
30

31 **References**

- 32
33
34 [1] D.M. Rowe, Thermoelectrics handbook: macro to nano. CRC press. 80, 2005
35 [2] T. Hendricks, W.T. Choate, Engineering scoping study of thermoelectric generator systems
36 for industrial waste heat recovery, US Dep. Energy. 20 (2006) 74.
37 [3] Z. Ouyang, D. Li, Sci. Rep. 6 (2016) 24123.
38 [4] G.J. Snyder, , Appl. Phys. Lett. 84 (2004) 2436–2438.
39 [5] M.S. El-Genk, H.H. Saber, AIP Conf. Proc. 699 (2004) 230.
40 [6] A.A. Usenko, D.O. Moskovskikh, M. V. Gorshenkov, A. V. Korotitskiy, S.D. Kaloshkin,
41 A.I. Voronin, V. V. Khovaylo, Scr. Mater. 96 (2015) 9–12.
42 [7] A. Usenko, D. Moskovskikh, M. Gorshenkov, A. Voronin, A. Stepashkin, S. Kaloshkin, D.
43 Arkhipov, V. Khovaylo, Scr. Mater. 127 (2017) 63–67.
44 [8] P. Bellanger, S. Gorsse, G. Bernard-Granger, C. Navone, A. Redjaimia, S. Vivès, Acta
45 Mater. 95 (2015) 102–110.
46 [9] D.B. Xiong, N.L. Okamoto, H. Inui, Enhanced thermoelectric figure of merit in p-type Ag-
47 doped ZnSb nanostructured with Ag₃Sb, Scr. Mater. 69 (2013) 397–400.
48 [10] L.P. Bulat, V.B. Osvenskii, D.A. Pshenay-Severin, Mater. Today Proc. 2 (2015) 532–537.
49
50
51
52
53
54
55
56
57
58
59
60
61
62
63
64
65

- 1
2
3
4
5
6
7
8
9
10
11
12
13
14
15
16
17
18
19
20
21
22
23
24
25
26
27
28
29
30
31
32
33
34
35
36
37
38
39
40
41
42
43
44
45
46
47
48
49
50
51
52
53
54
55
56
57
58
59
60
61
62
63
64
65
- [11] D. Berthebaud, T. Nishimura, T. Mori, *J. Mater. Res.* 25 (2010) 665–669.
 - [12] A.T. Burkov, S. V. Novikov, V. V. Khovaylo, J. Schumann, *J. Alloys Compd.* 691 (2017) 89–94.
 - [13] C. Bera, M. Soulier, C. Navone, G. Roux, J. Simon, S. Volz, N. Mingo, *J. Appl. Phys.* 108 (2010) 124306.
 - [14] X.W. Wang, H. Lee, Y.C. Lan, G.H. Zhu, G. Joshi, D.Z. Wang, J. Yang, A.J. Muto, M.Y. Tang, J. Klatsky, S. Song, M.S. Dresselhaus, G. Chen, Z.F. Ren, *Appl. Phys. Lett.* 93 (2008) 193121.
 - [15] S. Bathula, M. Jayasimhadri, N. Singh, A.K. Srivastava, J. Pulikkotil, A. Dhar, R.C. Budhani, *Appl. Phys. Lett.* 101 (2012) 213902.
 - [16] D.J. Bergman, L.G. Fel, *J. Appl. Phys.* 85 (1999) 8205–8216.
 - [17] N. Mingo, D. Hauser, N.P. Kobayashi, M. Plissonnier, A. Shakouri, *Nano Lett.* 9 (2009) 711–715.
 - [18] E.R. Johnson, S.M. Christian, *Phys. Rev.* 95 (1954) 560–561.
 - [19] Z. Zamanipour, D. Vashaee, *J. Appl. Phys.* 112 (2012) 1–9.
 - [20] P. Rouhani, Z. Zamanipour, J.S. Krasinski, D. Vashaee, L. Tayebi, 2012 IEEE Green Technol. Conf. (2012) 1–4.
 - [21] A. Usenko, D. Moskovskikh, A. Korotitskiy, M. Gorshenkov, A. Voronin, D. Arkhipov, M. Lyange, G. Isachenko, V. Khovaylo, *J. Electron. Mater.* 45 (2016) 3427–3432.
 - [22] F.W. Dynys, A. Sayir, J. Mackey, A. Sehirlioglu, *J. Alloys Compd.* 604 (2014) 196–203.
 - [23] K. Favier, G. Bernard-Granger, C. Navone, M. Soulier, M. Boidot, J. Leforestier, J. Simon, J.C. Tedenac, D. Ravot, *Acta Mater.* 64 (2014) 429–442.
 - [24] S. Ahmad, A. Singh, A. Bohra, R. Basu, S. Bhattacharya, R. Bhatt, K.N. Meshram, M. Roy, S.K. Sarkar, Y. Hayakawa, A.K. Debnath, D.K. Aswal, S.K. Gupta, *Nano Energy.* 27 (2016) 282–297.
 - [25] A. Nozariasbmarz, P. Roy, Z. Zamanipour, J.H. Dycus, M.J. Cabral, J.M. LeBeau, J.S. Krasinski, D. Vashaee, *APL Mater.* 4 (2016) 104814.
 - [26] J. Garg, N. Bonini, B. Kozinsky, N. Marzari, *Phys. Rev. Lett.* 106 (2011) 45901.
 - [27] R.M. German, *Liquid phase sintering*, Springer Science & Business Media, 2013.
 - [28] S. Bathula, M. Jayasimhadri, B. Gahtori, N.K. Singh, K. Tyagi, A.K. Srivastava, A. Dhar, *Nanoscale.* 7 (2015) 12474–12483.

Table 1: Sintering parameters and volume density of n -type $\text{Si}_{0.9}\text{Ge}_{0.1}\text{-Mg}_2\text{Si}$ nanocomposites

1
2
3
4
5
6
7
8
9
10
11
12
13
14
15
16
17
18
19
20
21
22
23
24
25
26
27
28
29
30
31
32
33
34
35
36
37
38
39
40
41
42
43
44
45
46
47
48
49
50
51
52
53
54
55
56
57
58
59
60
61
62
63
64
65

Fig. 1 XRD patterns collected for n -type $\text{Si}_{0.9}\text{Ge}_{0.1}\text{-Mg}_2\text{Si}$ 10% (at.): a) powder, b) spark plasma sintered and c) annealed sample

Fig. 2 SEM image and EDS elemental mapping of Si, Mg and Ge of bulk $\text{Si}_{0.9}\text{Ge}_{0.1}\text{-Mg}_2\text{Si}$ 10% (at.) nanocomposite after annealing

Fig. 3 Total (a), electronic (b) and lattice (c) thermal conductivities of sintered $\text{Si}_{0.9}\text{Ge}_{0.1}\text{-Mg}_2\text{Si}$ nanocomposites, reference RTG sample [1] and bulk nanostructured $\text{Si}_{0.8}\text{Ge}_{0.2}$ sample [6]

Fig. 4 Temperature dependence of the electrical conductivity (a), Seebeck coefficient (b) and ZT (c) of sintered $\text{Si}_{0.9}\text{Ge}_{0.1}\text{-Mg}_2\text{Si}$ nanocomposites, reference RTG sample [1] and bulk nanostructured $\text{Si}_{0.8}\text{Ge}_{0.2}$ sample [6]

Table 1: Sintering parameters and volume density of *n*-type Si_{0.9}Ge_{0.1}-Mg₂Si nanocomposites

Sample	Sintering temperature, °C	Soaking time, min	Pressure, MPa	Heating rate, °C/min	Density, % of theoretical
Si _{0.9} Ge _{0.1}	1150	5	65	75	98.81
Si _{0.9} Ge _{0.1} – Mg ₂ Si 1% (at.)	1100	5	65	75	98.53
Si _{0.9} Ge _{0.1} – Mg ₂ Si 3% (at.)	1065	5	65	75	95.12
Si _{0.9} Ge _{0.1} – Mg ₂ Si 10% (at.)	1045	5	65	75	93.97

Figure 1
[Click here to download high resolution image](#)

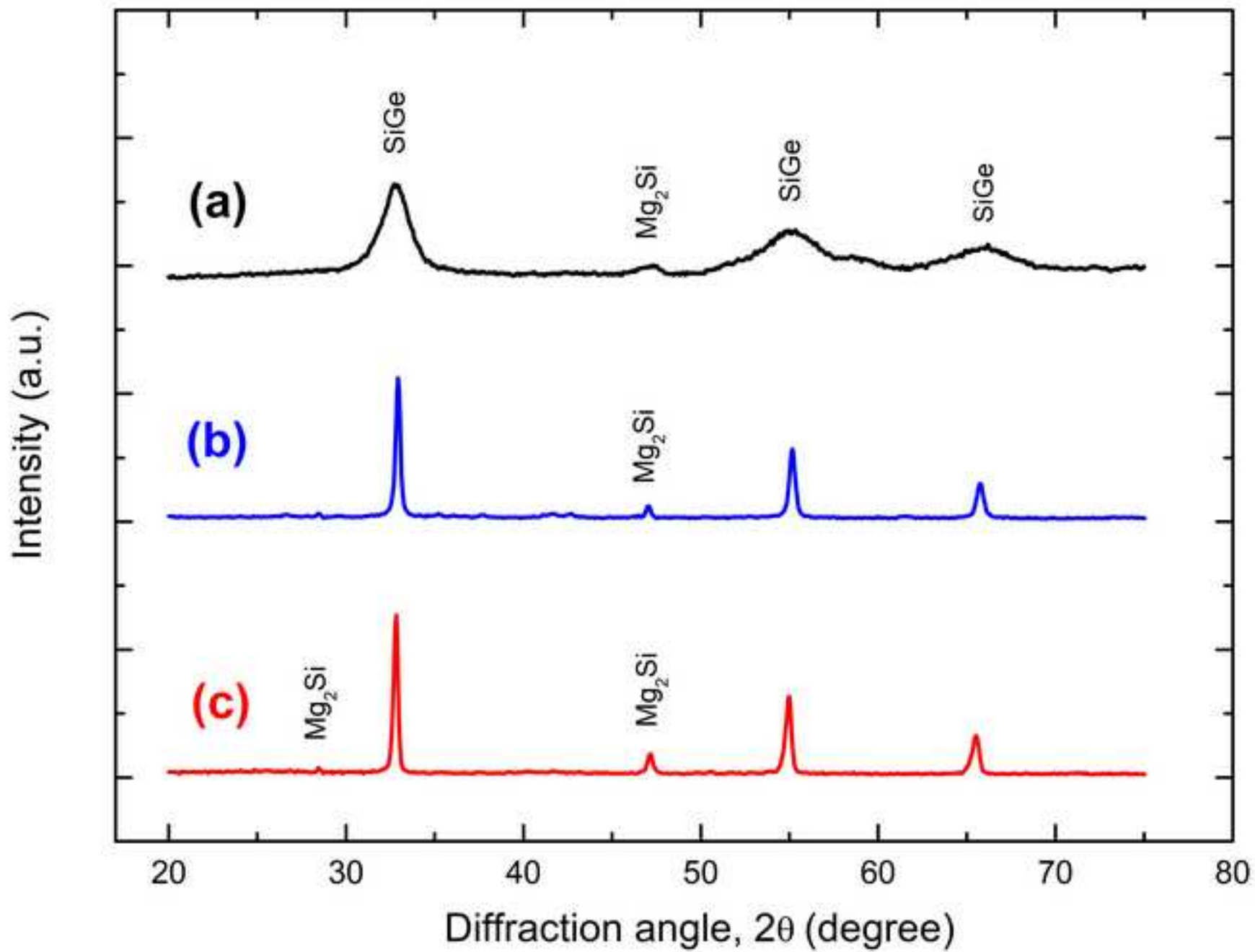


Figure 2
[Click here to download high resolution image](#)

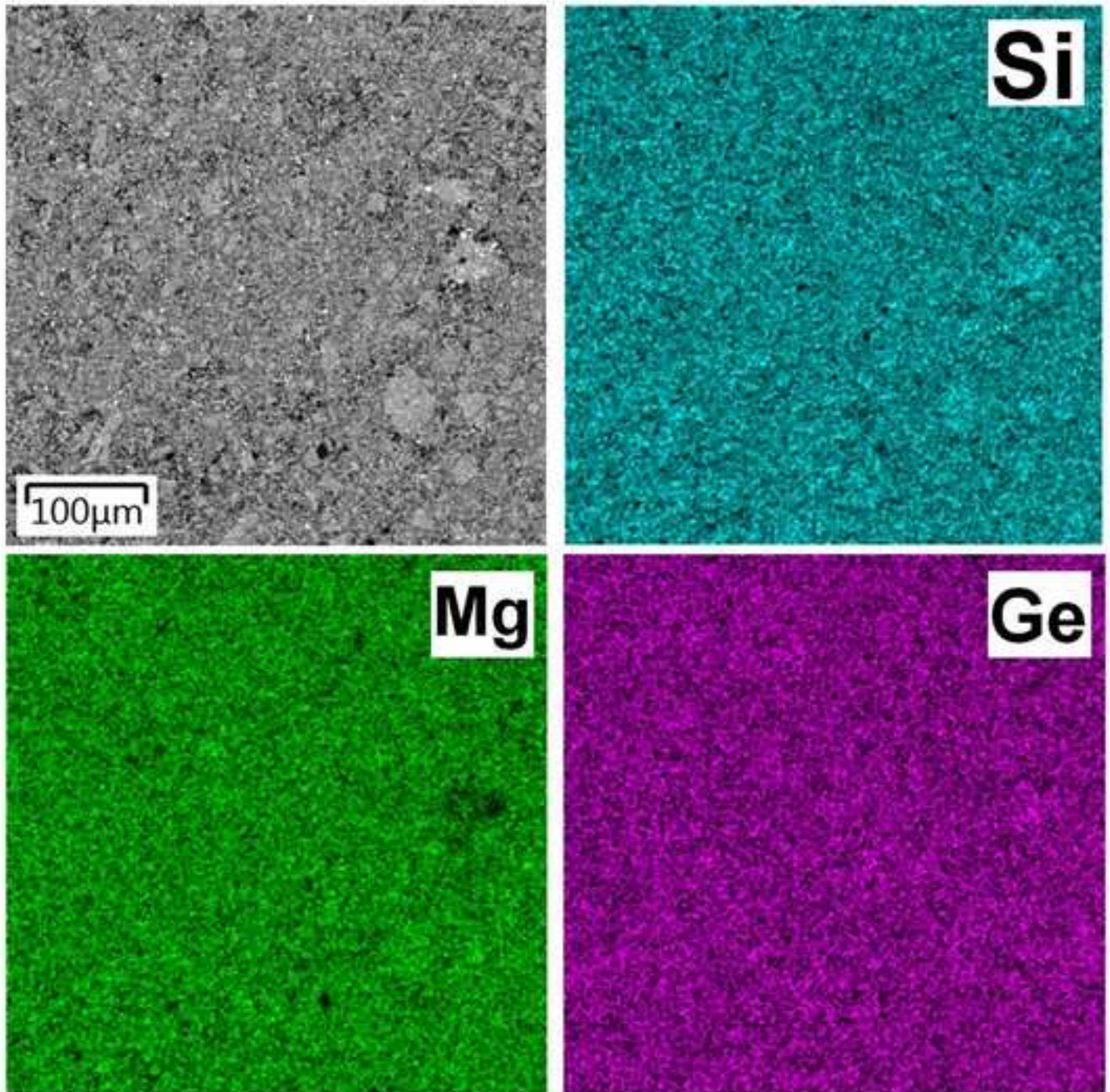


Figure 3
[Click here to download high resolution image](#)

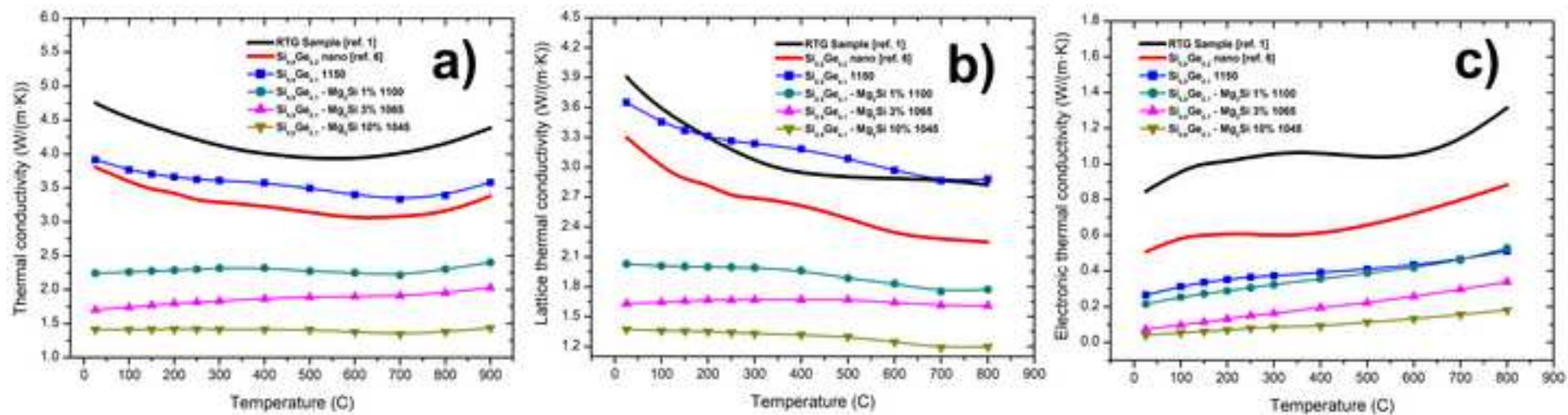


Figure 4

[Click here to download high resolution image](#)

